THE FASEB JOURNAL • RESEARCH • www.fasebj.org

Facilitation of MrgprD by TRP-A1 promotes neuropathic pain

Changming Wang,[*,†,‡,§] Leying Gu,[*,†,‡,§] Yonglan Ruan,[*,†,‡,§] Xiao Geng,[*,†,‡,§] Miao Xu,[¶] Niuniu Yang,[*,‖] Lei Yu,[*,†] Yucui Jiang,[*,†] Chan Zhu,[*,†,‡,§] Yan Yang,[*,†,‡,§] Yuan Zhou,[*,†,‡,§] Xiaowei Guan,[*,†,‡,§] Wenqin Luo,[#] Qin Liu,[,††,‡‡] Xinzhong Dong,[§§,¶¶] Guang Yu,[*,†,‡,§,1] Lei Lan,[¶,2] and Zongxiang Tang[*,†,‡,§]**

[*]School of Medicine and Life Sciences, [†]Key Laboratory of Chinese Medicine for Prevention and Treatment of Neurological Diseases, [‡]State Key Laboratory Cultivation Base for Traditional Chinese Medicine Quality and Efficacy, and [§]Key Laboratory of Drug Target and Drug for Degenerative Disease of Jiangsu Province, Nanjing University of Chinese Medicine, Nanjing, China; [¶]Jiangsu Province Key Laboratory for Molecular and Medical Biotechnology, College of Life Sciences, Nanjing Normal University, Nanjing, China; [‖]Department of Traditional Chinese and Western Medicine, Jiangsu Key Laboratory of Integrated Traditional Chinese and Western Medicine for Prevention and Treatment of Senile Diseases, Yangzhou University, Yangzhou, China; [#]Department of Neuroscience, Perelman School of Medicine, University of Pennsylvania, Philadelphia, Pennsylvania, USA; [**]Department of Anesthesiology, [††]Center for the Study of Itch, and [‡‡]Department of Ophthalmology and Visual Sciences, Washington University School of Medicine, St. Louis, Missouri, USA; and [§§]The Solomon H. Snyder Department of Neuroscience, Center for Sensory Biology, and [¶¶]Howard Hughes Medical Institute, School of Medicine, Johns Hopkins University, Baltimore, Maryland, USA

ABSTRACT: Neuropathic pain remains a therapeutic challenge because of its complicated mechanisms. Mas-related GPCR D (MrgprD) is specifically expressed in small-diameter, nociceptive neurons of dorsal root ganglia (DRGs) and is implicated in pain modulation. However, the underlying mechanism of MrgprD involved in neuropathic pain remains elusive. In this study, we used behavioral experiments and physiologic examination methods to investigate the role of MrgprD in chronic constriction injury (CCI)–induced neuropathic pain. We found that MrgprD is necessary for the initiation of mechanical hypersensitivity and cold allodynia, but not for heat allodynia. Moreover, we demonstrated that transient receptor potential cation channel (TRP)-A1 was the ion channel downstream of MrgprD, and the β-alanine–induced calcium signal was attributed mostly to TRP-A1 function. We further showed that PKA serves as a downstream mediator of β-alanine–activated MrgprD signaling to activate TRP-A1 in DRG neurons and in human embryonic kidney 293 cells, to coexpress MrgprD and TRP-A1 plasmids. Finally, we found that the β-alanine–induced pain behavior was increased, whereas the itching behavior was unchanged in CCI models compared with sham-injured animals. Knockout of *TRPA1* also attenuated the β-alanine–induced pain behavior in CCI models. In conclusion, MrgprD is essential in cold allodynia in CCI-induced neuropathic pain through the PKA–TRP-A1 pathway. TRP-A1 facilitates MrgprD to development of neuropathic pain. Our findings reveal a novel mechanism of neuropathic pain formation and highlight MrgprD as a promising drug target for the treatment of neuropathic pain.—Wang, C., Gu, L., Ruan, Y., Geng, X., Xu, M., Yang, N., Yu, L., Jiang, Y., Zhu, C., Yang, Y., Zhou, Y., Guan, X., Luo, W., Liu, Q., Dong, X., Yu, G., Lan, L., Tang, Z. Facilitation of MrgprD by TRP-A1 promotes neuropathic pain. FASEB J. 33, 1360–1373 (2019). www.fasebj.org

KEY WORDS: MrgprA1 · dorsal root ganglia (DRG) · protein kinase A (PKA)

Neuropathic pain arises as a direct consequence of a lesion or disease that affects the somatosensory system, either at the peripheral or central level (1, 2). It causes suffering and disability, such as trauma, neuronal injury, or infection (3), and afflicts 6.9–10% of the population worldwide, with continually increasing numbers (4). The mechanisms of neuropathic pain are far from being fully understood. Because of its high clinical morbidity and complex etiology, neuropathic pain remains a pressing challenge to researchers.

One mechanism that has been proposed to mediate the sensitization and activation of pain stimuli involves

ABBREVIATIONS: CCI, chronic constriction injury; DRG, dorsal root ganglion; EGFP, enhanced green fluorescent protein; HEK, human embryonic kidney; HEPES, 4-(2-hydroxyethyl)-1-piperazineethanesulfonic acid; MrgprD, Mas-related GPCR D; MWT, mechanical withdrawal threshold; TRP, transient receptor potential; TWL, thermal withdrawal latency; WT, wild type

[1] Correspondence: Nanjing University of Chinese Medicine, 138 Xianlin Rd., Nanjing 210023, Jiangsu, China. E-mail: yuguang928@126.com

[2] Correspondence: Jiangsu Province Key Laboratory for Molecular and Medical Biotechnology, College of Life Sciences, Nanjing Normal University, Nanjing, 210046, Jiangsu, China. E-mail: lanlei@njnu.edu.cn

doi: 10.1096/fj.201800615RR

This article includes supplemental data. Please visit *http://www.fasebj.org* to obtain this information.

0892-6638/19/0033-1360 © FASEB

GPCRs, which may function with transient receptor potential (TRP) channels to detect noxious, irritating, and inflammatory stimuli. Signals emanating from the GPCR superfamily are amplified by the TRP channels, and these 2 classes of molecules are coexpressed in subclasses of neurons (5). Mas-related GPCR D (MrgprD; also known as MrgD or TGR7) is a GPCR that is expressed within $IB4^+$ dorsal root ganglion (DRG) neurons and has been proposed to be involved in pain sensation and modulation (6, 7). Several studies have reported that β-alanine, a specific agonist of MrgprD, evokes Ca^{2+} influx (7–9), indicating that MrgprD functions as one of the components in the GPCR–TRP axis.

MrgprD-knockout ($MrgprD^{-/-}$) mice were generated to elucidate the mechanisms of MrgprD in pain sensation (10); however, the mice did not exhibit any nociceptive sensory differences, such as thermal or mechanical deficits compared with their wild-type (WT) littermates (9). Instead, MrgprD has been thought to mediate β-alanine–elicited itching, which declines significantly in $MrgprD^{-/-}$ mice (9, 11). Although recent research efforts have focused on the role of MrgprD in itching (9, 11), the role of MrgprD in neuropathic pain and the underlying mechanisms are largely unknown.

In the present study, we investigated in detail the role of MrgprD in neuropathic pain in a chronic constriction injury (CCI) mouse model. We found that the CCI-induced behavioral hypersensitivities to mechanical and cold stimuli, but not to heat stimulus, were substantially decreased in $MrgprD^{-/-}$ mice compared with WT littermates. We further investigated whether and how MrgprD functions together with cold-sensing TRP channels in the periphery. We revealed that β-alanine–induced MrgprD activation evoked calcium influx, which was highly associated with the activity of TRP-A1 and was attenuated in TRP-A1–knockout mice. We also showed that the inhibitor of PKA can substantially suppress the β-alanine–induced calcium increase in DRG neurons. β-Alanine–induced pain behavior increased in the CCI models, but was attenuated in the TRP-A1–knockout mice in the CCI model.

We demonstrated that MrgprD is essential for the initiation of mechanical hypersensitivity and cold allodynia in the CCI mouse model and is functionally associated with TRP-A1 through PKA. The administration of β-alanine mainly induced pain behavior in animals under neuropathic pain conditions.

MATERIALS AND METHODS

Animals

This study was approved by the Animal Care and Use Committee of Nanjing University of Chinese Medicine (Nanjing, China). Experiments were conducted according to the animal research ethics guidelines of the International Association for the Study of Pain. Male C57BL/6 mice were housed in groups of 4 per cage in our animal center, with free access to food and water and a controlled temperature (22 ± 4°C). Under an automatically controlled light cycle, mice were kept in alternating 12 h periods of light and dark. For the generation of $MrgprD^{-/-}$ mice, the entire open reading frame of MrgprD was replaced with an in-frame fusion of enhanced green fluorescent protein (EGFP) (10). $MrgprD^{-/-}$ mice were backcrossed 7 times in the C57BL/6 background, and $MrgprD^{+/+}$ C57BL/6J mice were used as controls. Offspring $MrgprD^{-/-}$ and $MrgprD^{+/+}$ littermate controls were generated by breeding heterozygotes. For the generation of $TRPA1^{-/-}$ mice, the essential exons necessary for proper function of the TRP-A1 gene were deleted (12). $TRPA1^{-/-}$ mice were backcrossed 7 times in the C57BL/6 background, and $TRPA1^{+/+}$ C57BL/6J mice were used as controls. Offspring $TRPA1^{-/-}$ and $TRPA1^{+/+}$ littermate controls were generated by breeding heterozygotes. Only healthy animals weighing 15–20 g and displaying normal water and food intake were included in the study. All behavioral tests were performed by an experimenter blind to the groups.

CCI

Mice were anesthetized with 1% pentobarbital sodium (40 mg/kg; Merck, Darmstadt, Germany) and restrained in a lateral position. A surgical incision was made at the thigh root midline, and the right sciatic nerve was exposed at the middle of the thigh. Three ligatures were tied around the nerve with 5-0 silk braided cord (Shanghai Pudong Jinhuan Medical Products, Shanghai Shi, China) with a 1 mm space between each ligation point (13). The force of ligation was based on leg reflex. After the operation, the wounds were sutured closed, and the animals were positioned supine during injection and kept in that position until they recovered from anesthesia. A sham procedure was performed in the same manner, except that the sciatic nerve ligation was omitted. All surgical procedures were performed in sterile conditions.

Mechanical allodynia

Animals were acclimated to the testing environment for 30 min before the initiation of behavioral tests. Animal behavior was analyzed by investigators who were blind to the groups. Mechanical allodynia was assessed by measuring the paw withdrawal threshold with a set of Aesthesio Von Frey filaments (0.04–2 g; Ugo Basile, Gemonio, Italy). Mice were placed on an elevated metal grid (100 × 50 cm). The filament was applied to the plantar surface at a vertical angle for up to 3 s from the bottom. Fifty percent mechanical withdraw threshold (MWT) values were determined by using the up–down method (14).

Thermal hyperalgesia

Thermal hyperalgesia was assessed by measuring the paw withdrawal latency to radiant heat stimuli after the Von Frey test. Hind paw withdrawal latency was measured by the method of Hargreaves *et al.* (15). Mice were placed in elevated chambers on a Plexiglas floor and acclimated to the testing environment for 30 min before the experiments. The radiant heat source (plantar test, 37370; Ugo Basile, SRL, Gemonio, Italy) was applied to the center of the plantar surface of the hind paw with intervals of at least 3 min between applications. The average thermal withdrawal latency (TWL) of the trials was recorded as the response latency.

Cold allodynia

Cold allodynia was evaluated by the acetone test (12, 16). Mice were placed on an organic glass plate (100 × 50 cm). A drop (50 μl) of acetone was applied to the midplantar area of the hind paw, and the resulting behavior was monitored over a period of 1 min. The score was used to measure the extent of the animal's reaction (0, no response; 1, quick withdrawal or flicking; 2, prolonged

withdrawals or repeated flicking of the paw; and 3, repeated flicking of the paw with licking of the paw). Acetone was applied 3 times to each paw alternately, and the responses were scored. Cumulative scores were then obtained by adding the 3 scores for each of the mice.

Culture of primary neurons

The mice were anesthetized with 1% pentobarbital sodium. The DRGs were harvested as described by Wang *et al*. (17) and immediately transferred to cold DH10 medium [DMEM/F-12, 10% fetal bovine serum (Thermo Fisher Scientific, Waltham, MA, USA), 1% penicillin-streptomycin-glutamine (Solarbio, Beijing, China)]. DRGs were washed 2–3 times in warm DH10 and then treated with enzyme solution (5 mg/ml Dispase and 1 mg/ml collagenase type I in HBSS without Ca^{2+} and Mg^{2+}; Thermo Fisher Scientific) at 37°C until the cells were dissociated (18, 19). Cell suspensions were then filtered through a 100 μm cell strainer (BD Bioscience, Franklin Lakes, NJ, USA). After being centrifuged at 1000 rpm for 5 min, DRG neurons were resuspended in DH10, and nerve growth factor (50 ng/ml; MilliporeSigma, Burlington, MA, USA) was added. Fifty microliters of cells suspended in solution were plated on presterilized glass cover slips that had been coated with 0.5 mg/ml poly-D-lysine (Thermo Fisher Scientific) and 10 μg/ml laminin (MilliporeSigma). Plated neurons were cultured in an incubator (95% O_2 and 5% CO_2) at 37°C and used for calcium imaging studies within 48 h.

Human embryonic kidney 293 cell culture

Human embryonic kidney (HEK) 293 cells were cultured on presterilized glass cover slips that had been coated with 0.5 mg/ml poly-D-lysine (Biomedical Technologies) and 10 μg/ml laminin (Thermo Fisher Scientific). Cells were transfected with Lipofectamine 2000 (Thermo Fisher Scientific) using 150 ng human MrgprD and TRP-A1 plasmids. The cells were planted on glass cover slips. Sixteen hours after transfection, the cover slips were moved into the perfusion chamber and used for calcium imaging.

Calcium imaging assay

The DRG neurons were loaded with fura-2-acetoxymethylester (Thermo Fisher Scientific) for 30 min at 37°C in the dark in accordance with the previous studies (17–19). After they were washed 3 times with PBS, the cover slips were placed in a chamber and perfused with a calcium imaging buffer containing 137 mM NaCl, 5.4 mM KCl, 1.2 mM $MgCl_2$, 1.2 mM NaH_2PO_4, 1 mM $CaCl_2$, 8 mM glucose, and 20 mM 4-(2-hydroxyethyl)-1-piperazineethanesulfonic acid (HEPES; pH 7.4). The calcium-free imaging buffer contained 137 mM NaCl, 5.4 mM KCl, 1.2 mM $MgCl_2$, 1.2 mM NaH_2PO4, 8 mM EDTA, 8 mM glucose, and 20 mM HEPES (pH 7.4). A high-speed, continuously scanning, monochromatic light source (Polychrome V; Till Photonics, Gräfeling, Germany) was used for excitations of 340 and 380 nm, enabling the detection of changes in the intracellular free-calcium concentration. Cells were considered responsive if the fluorescence ratio ≥0.4 (fluorescence ratio = $\Delta F - F_0$, where ΔF is the maximum value of fluorescence − baseline fluorescence; F_0 is the baseline fluorescence). Cells were considered inhibited if the fluorescence ratio of β-alanine–induced calcium influx decreased when perfused with enzyme inhibitor to the level of two-thirds of intensity of β-alanine stimulation alone. All calcium imaging assays were performed by an experimenter blind to the groups (17).

Whole-cell patch-clamp recording

In voltage clamp recordings, currents were detected with an Axon 700B amplifier and the pCLAMP 10.1 software package (Molecular Devices, Sunnyvale, CA, USA). Cells were bathed in normal solution (in mM): 140 NaCl, 4 KCl, 2 $CaCl_2$, 2 $MgCl_2$, 10 HEPES, 5 glucose, adjusted to pH 7.4 with NaOH. Pipette resistance ranged from 2 to 5 MΩ. The internal solution (in mM) was 35 KCl, 3 MgATP, 0.5 Na_2ATP, 1.1 $CaCl_2$, 2 EGTA, 5 glucose, adjusted to pH 7.4 with KOH and 300 mOsmol osmolarity with sucrose. Capsaicin was stored at −20°C and diluted to 1 μM in the extracellular solution. Electrodes (model P-97; Sutter, Novato, CA, USA) were seated in borosilicate glass (Molecular Devices). All experiments were performed at room temperature.

Immunofluorescence and immunostaining of DRG neurons

DRG tissues were collected from spine levels L4–L5. The DRGs were then embedded in optimum cutting temperature compound (OCT; Leica, Wetzlar, Germany) and rapidly frozen at −20°C (CM1950; Leica). Cryoembedded tissues were cut into 10 μm–thick slices on a sliding microtome (CM1950; Leica). DRG neurons from $MrgprD^{-/-}$ mice can display florescence because a fused in-frame EGFP fluorescence of the gene was inserted on the MrgprD site. (10). For immunostaining of TRP-A1, sections were incubated in blocking solution (containing 3% FBS, 0.1% Triton X-100, and 0.02% sodium azide in PBS) for 2 h at room temperature and then with rabbit anti-TRP-A1 (1:100, ab62053; Abcam, Cambridge, United Kingdom) at 4°C overnight. Next, the sections were incubated in Alexa Fluor–conjugated goat anti-rabbit IgG secondary antibody (H+L, 1:100, A0453; Beyotime, Shanghai, China) at room temperature for 2 h. To calculate the positive cells in DRGs, every 2 slices were captured and counted. The number of fluorescing DRG neurons in L4 and L5 were counted and calculated. After stained pictures were captured, they were merged into an image. Three mice from each group were analyzed. Quantification of immunoreactivity was performed according to Ma *et al*. (20).

Real-time quantitative PCR

Total RNA was extracted from freshly isolated DRGs (L4–L5, S1–S2) with Trizol reagent (Thermo Fisher Scientific) and was treated with RQ1 DNAse (Promega Life Sciences, Madison, WI, USA). Reverse transcription was performed with the Transcript First Strand cDNA Synthesis kit (Roche, Basel, Switzerland).

For quantitative (q)PCR, Light Cycler 480 Sybr Green I Master mix (Roche) was used. The reaction was run in a Light Cycler 480 II Real-Time PCR instrument (Roche) with 1 μl of the cDNA in a 20 μl reaction according to the manufacturer's instructions. The sequences of the mouse primers were MrgprD forward, 5′-TTTTCAGTGACATTCCTCGCC-3′, reverse, 5′-GCACATAGACACAGAAGGGAGA-3′; TRP-A1 forward, 5′-GTCCAGGGCGTTGTCTATCG-3′, reverse, 5′-CGTGATGCAGAGGACAGAGAT-3′; and GAPDH forward, 5′-ACCACAGTCCATGCCATCAC-3′, reverse, 5′-TCCACCACCCTGTTGCTGTA-3′. Calibrations and normalizations were performed with the following $2^{-\Delta\Delta CT}$ method: where ${}^{\Delta\Delta}C_t$ = [CT (target gene) − CT (reference gene)] − [CT (calibrator) − CT (reference gene)]. GAPDH was used as the reference gene for real-time qPCR experiments.

Protein extraction and Western blot analysis

Total protein from freshly dissected DRGs (L4–L5 and S1–S2) was isolated and purified with Trizol/chloroform and an

isopropanol precipitation procedure, in accordance with the manufacturer's protocols (Thermo Fisher Scientific). The protein concentration was determined by bicinchoninic assay. β-Actin was selected as an internal control. pAb of MrgprD (Neuromics, Edina, MN, USA) was used at 1:500 dilution and an mAb of β-actin (Santa Cruz Biotechnology, Dallas, TX, USA) was used at 1:1000 dilution. Equal quantities of protein (60 μg/lane) were resolved on 12% SDS-polyacrylamide gels. The intensity of the signals was used to estimate the relative concentration of TRP-A1 protein in the DRG extracts.

Nanoimmunoassay

A nanoimmunoassay involves separation of cell lysates, in the capillary isoelectric focusing step, and analysis of protein phosphorylation (NanoPro 1000 system; Protein Simple, Wallingford, CT, USA). Cultured DRG neurons were pretreated with β-alanine (8 mM, 5 min) or H89 (1 μM) in 24-well plates (1×10^5 cells) and homogenized in 500 μl bicine/3-(3-cholamidopropyl) dimethylammonio)-1-propanesulfonate lysis buffer (040–764; Protein Simple) plus 10 μl dimethyl sulfoxide inhibitor mix (040–510; Protein Simple) and 20 μl aqueous inhibitor mix (040–482; Protein Simple). The cell lysates were cleared by centrifugation at 18,000 rpm for 1 h at 4°C (M0290S; New England Biolabs, Ipswich, MA, USA) at 37°C for 1 h. The supernatants were diluted to 1000 μg/μl by sample diluents (040–649; Protein Simple) in the presence of a DMSO inhibitor mix (040–510; Protein Simple). Diluted supernatants were combined with Premix G2 (040–968; Protein Simple) and a pI standard ladder 1 (040–968; Protein Simple). The charge-based separation was performed in a capillary at 45,000 W for 40 min. Immobilization was conducted with 100 s of irradiation with UV light. The sample was incubated with the TRP-A1 antibody used in the immunofluorescence analysis for 120 min after separation and immobilization. It was then incubated with biotin-conjugated goat anti-mouse (041–127 or 041–126; Protein Simple) for 1 h followed by 10 min of incubation with streptavidin-conjugated horseradish peroxidase. Chemiluminescence signals for the target proteins were detected by adding luminol (040–652; Protein Simple) and peroxide XDR detection reagents (041–084; Protein Simple). They were then analyzed with Compass software (Compass Software, Dortmund, Germany).

Intradermal injection of β-alanine

Intraplantar injection of β-alanine (50 mM, 10 μl) in mice, the behavioral responses of licking and biting were video recorded with a 4 K camera. The video recordings were played back for measurements of the responses. For the calf model, the number of times licking and biting were recorded for 20 min. Licking behavior and biting behavior were counted as described in refs. 11 and 21–23. For the cheek model, β-alanine (50 mM, 10 μl) was injected intradermally into the cheek and a behavioral response video was recorded for 20 min. The video recordings were subsequently viewed to extract the number of bouts of scratching and the number of wipes directed toward the site of the injection, as described in ref. 11 and 24.

Data analysis

All data are presented as means ± SEM. The number of animals used in each study was based on our experience and on similar studies. Experimenters were blinded to the genotype of mice and different groups, to reduce selection and observation bias. After the experiments were completed, no data point was excluded. The littermate controls were used for behavioral tests of pain and itch behavior, and the results were analyzed by paired sample *t* tests. (The WT and knockout mice of the same mother and the same day of birth made up a pair.) For morphologic results, we used representative data from 3 mice with similar results. Statistical analysis of the number of $MrgprD^+$ cells and $TRP\text{-}A1^+$ cells were performed manually. We used representative data from Ca^{2+} imaging studies that were replicated at least 15 times from 3 mice (5 times in each mouse). The different tests used in data analysis are shown in the figure legends. Values of $P < 0.05$ were considered statistically significant in all tests.

RESULTS

MrgprD is necessary in the mechanical and cold allodynia in the CCI model

To determine whether MrgprD participates in CCI-induced neuropathic pain, we administered CCI or sham CCI to $MrgprD^{-/-}$ mice and WT mice, respectively, and then recorded the MWTs and TWLs on d 1, 3, 5, 7, 9, 11, and 13 after the operation. We did not observe any significant differences in the MWT values without CCI between WT and $MrgprD^{-/-}$ mice (Supplemental Fig. 1*A*). By contrast, after CCI, the MWTs of WT mice were significantly lower than those of $MrgprD^{-/-}$ mice (**Fig. 1*A*, *B***), suggesting that MrgprD participates in mechanical allodynia in the CCI model. However, $MrgprD^{-/-}$ mice responded normally to heat stimulus compared with WT mice (Fig. 1*C*, *D*).

We further used an acetone test to determine whether MrgprD is involved in CCI-induced cold allodynia. Although there was no significant difference between $MrgprD^{-/-}$ mice and WT mice without CCI (Supplemental Fig. 1*C*), the cold responses in the ipsilateral paws were significantly lower in $MrgprD^{-/-}$ mice than those in CCI WT mice (Fig. 1*E*, *F*). These observations suggest that MrgprD is essential in maintaining the mechanical and cold allodynia, but not heat allodynia in CCI-induced neuropathic pain.

MrgprD is up-regulated in CCI mice

To investigate the involvement of MrgprD in CCI-induced neuropathic pain, we first determined the expression of MrgprD. In $MrgprD^{-/-}$ mice, the coding region of *MrgprD* was replaced with an *EGFP* gene, as described by Wang *et al*. (17). Taking advantage of EGFP, the DRG neurons specifically expressing MrgprD can be visualized by imaging GFP fluorescence in $MrgprD^{+/-}$ mice. As shown in **Fig. 2*A–C***, in comparison with DRGs from naive or sham-CCI $MrgprD^{+/-}$ mice, the percentage of $EGFP^+$ neurons was increased in DRGs from CCI mice (Fig. 2*D*,1037 $MrgprD^+$ cells in 2979 DRG neurons in the CCI group and 814 $MrgprD^+$ cells in 2645 DRG neurons in the naive group). Consistently, the expression of *MrgprD* at transcription level in CCI WT mice was increased, as determined by real-time PCR (Fig. 2*E*). These observations indicated that CCI induced the up-regulation of MrgprD in DRG neurons. It is known that β-alanine is one of the agonists of MrgprD and can induce an intracellular calcium increase in 15% of DRG neurons (9, 11, 25). Then, we discriminated the origin of β-alanine–induced calcium by using calcium imaging buffer, with or without calcium chloride. As shown in Supplemental Fig. 2*E*, the β-alanine–induced calcium influx occurred in a dose-dependent manner ($EC_{50} \approx 8$ mM) in DRG neurons of WT mice. Moreover, the

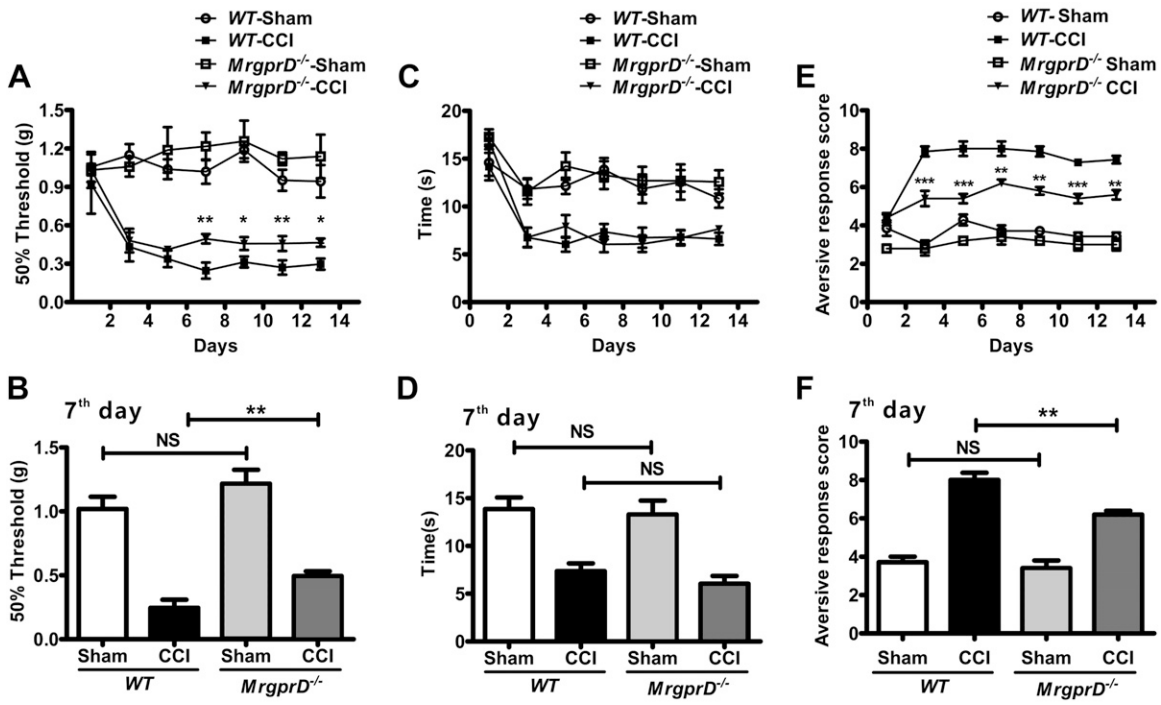

Figure 1. The behavioral differences between WT and *MrgprD*$^{-/-}$ mice. *A*) Von Frey testing during 14 d on WT and *MrgprD*$^{-/-}$ mice after CCI or sham injury (control). Values represent the changes from the baseline MWTs that were recorded on d 0 after CCI. *B*) The MWTs on d 7 after CCI. *C*) Radiant heat stimulus testing over 14 d after CCI or sham injury. Values represent the change from the baseline TWL values that were recorded on d 0 after the procedure. *D*) The TWL values on the d 7 were compared. *E*) The cold responses in the ipsilateral paws of *MrgprD*$^{-/-}$ mice were significantly lower than that of WT mice during 14 d after CCI. *F*) The aversive response score of WT mice and *MrgprD*$^{-/-}$ mice in CCI models on d 7 ($n = 7$). $^{*}P < 0.05$, $^{**}P < 0.01$, $^{***}P < 0.001$, WT *vs.* *MrgprD*$^{-/-}$, by 2-way repeated-measures ANOVA, factorial design.

β-alanine–induced calcium signal totally disappeared when the calcium-containing buffer was changed to calcium-free buffer (Supplemental Fig. 2*A–D*), indicating that β-alanine–activated MrgprD signal affects a certain cation ion channel on the cell membrane. Furthermore, we examined the effects of CCI on the physiologic function of DRG neurons in WT mice. We counted the number of β-alanine–responsive neurons with different treatments by using a calcium-imaging assay, we found that the proportion of DRG neurons responding to β-alanine in CCI mice (23.1 ± 1.2%) was significantly higher than that in naive mice (14.9 ± 1.1%; Fig. 2*F*, 122 cells responded to β-alanine in 813 DRG neurons in the CCI group and 191 cells responded to β-alanine in 827 DRG neurons in the naive group in L4 and L5 DRGs), which is consistent with the increased number of MrgprD^{+} neurons after CCI. These results indicate that the expression levels of MrgprD are related to neuropathic pain in the CCI model.

MrgprD is colocalized with TRP-A1 in DRG neurons

As we observed above, the depletion of MrgprD resulted in the attenuation of cold allodynia, and it is thus possible that MrgprD is involved in the function of cold-sensing proteins, such as TRP-A1 ion channels. To test this hypothesis, we first determined the relationship between MrgprD and TRP-A1 in DRG neurons. By using a calcium imaging assay to determine neurons that were coresponsive to β-alanine and mustard oil, we found that, in 859 mustard oil–responsive and 344 β-alanine–responsive DRG neurons, there were 299 neurons that respond to both mustard oil and β-alanine. The percentage of coresponsive neurons in total was 13.07% (299/2287). Moreover, 86.92% of β-alanine–responsive neurons (299/344) were responsive to mustard oil (**Fig. 3*A, B, H***). Immunostaining further revealed that both MrgprD and TRP-A1 were coexpressed in a subset of DRG neurons (Fig. 3*C–F*), and the TRP-A1 antibody was effective in TRP-A1 KO DRGs (Fig. 3*C*). In Mrgpr^{+} neurons, 92.99% of cells expressed TRP-A1 (252/271). In TRP-A1^{+} neurons, 37.28% of cells expressed MrgprD (252/676) (Fig. 3*G*). Moreover, we detected the DRG neurons that were responsive to β-alanine and menthol (TRPM8 agonist). Finally, we found that fewer DRG neurons responded to both β-alanine and menthol (Supplemental Fig. 2*F*; $n = 3$ per group). These observations indicated that there is a functional relationship between MrgprD and TRP-A1 in DRG neurons.

β-Alanine–activated MrgprD signaling is coupled with TRP-A1 in cultured DRG neurons

To investigate the relationship between TRP-A1 and MrgprD, we examined the effect of the TRP-A1 inhibitor HC-030031 on the β-alanine–induced calcium influx. When HC-030031 (1 μM) was added to the perfusion buffer, the β-alanine (8 mM)–induced calcium influx was decreased. If the β-alanine stimulus was applied again, the

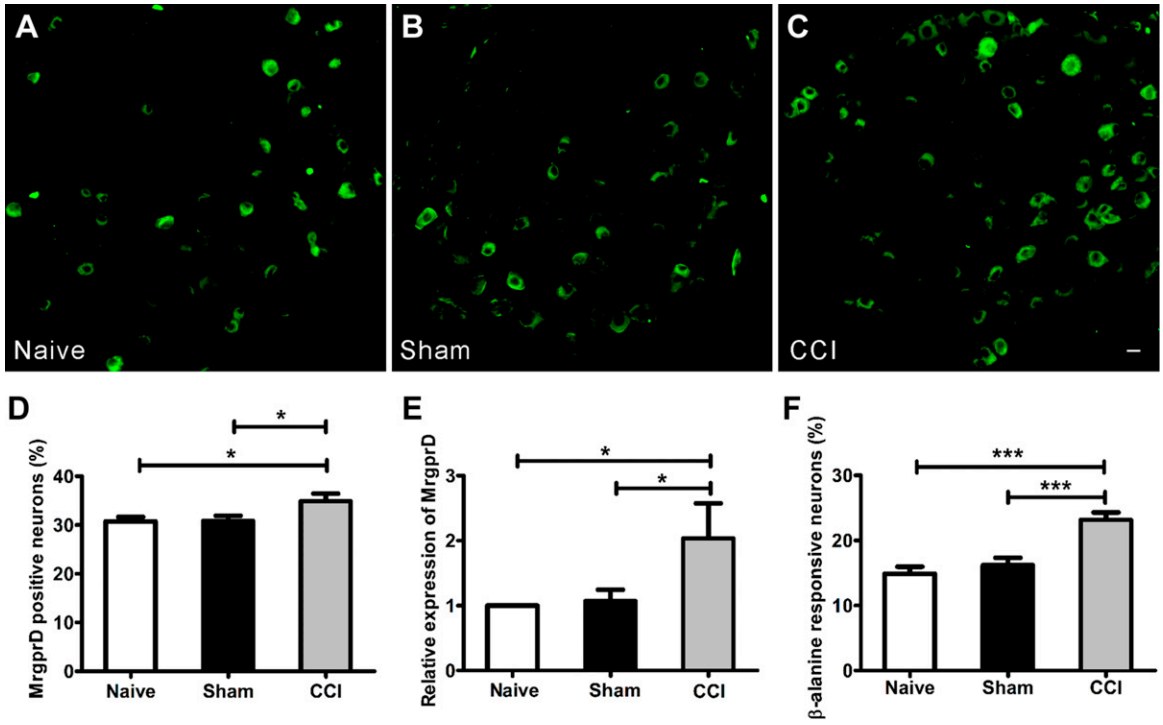

Figure 2. The expression of MrgprD increased in a CCI-induced neuropathic pain model. EGFP$^+$ neurons at the level of L4 DRGs were imaged in the naive (*A*), sham (*B*), and CCI (*C*) groups at d 14. Scale bar, 20 μm. *D*) The percentage of MrgprD$^+$ neurons in L4 DRGs. *E*) The results of real-time PCR show the up-regulated transcriptional expression of MrgprD in the CCI mice in comparison with the naive and sham-injured counterparts. *F*) The percentage of β-alanine–responsive neurons in L4 DRGs from the 3 groups (% of cultured neurons; $n = 3$ per group). $^*P < 0.05$, $^{***}P < 0.001$, by 1-way repeated-measures ANOVA.

response strength was restored (**Fig. 4*A*, *B***; 322 of 2150 DRG neurons responded to β-alanine, and 129 β-alanine–responsive cells were inhibited by HC-030031). Furthermore, we used whole-cell patch-clamp recording to validate the results of calcium imaging. Clearly, in the presence of HC-030031, the β-alanine–induced inward current was markedly decreased. Removal of HC-030031 resulted in the recovery of the β-alanine–induced response (Fig. 4*C*, *D*). We also examined the effect of the TRPM8 inhibitor RQ-00203078 on β-alanine–induced calcium influx. The inhibitory effect was not obvious compared with HC-030031 (Supplemental Fig. 2*G*, 1-way repeated measures ANOVA). Our data demonstrated that β-alanine–activated MrgprD signaling is coupled with TRP-A1 in DRG neurons.

The responses of β-alanine–induced MrgprD are attenuated in TRP-A1–knockout mice

To further explore the functional correlation between MrgprD and TRP-A1, we compared the responses of DRG neurons to β-alanine in WT and TRP-A1 knockout mice. The β-alanine–induced calcium influx was observed in the DRG neurons of the 2 types of animals (**Fig. 5*A***). The depletion of TRP-A1 caused decreases in both the intensity and the number of DRG neurons responsive to β-alanine (Fig. 5*B–D*; 164 cells responded to β-alanine in 1055 DRG neurons in the WT group, and 148 cells responded to β-alanine in 1741 DRG neurons in the *TRPA1*$^{-/-}$ group). These data further suggest that the presence of TRP-A1 could increase β-alanine–activated MrgprD responses. When the TRP-A1 agonist mustard oil was applied to activate DRG neurons from WT and *MrgprD*$^{-/-}$ mice, there were no significant differences in the number and intensity of cell responses (Fig. 5*E*, *F*; 355 cells responded to β-alanine in 995 DRG neurons in the WT group, and 339 cells responded to β-alanine in 1014 DRG neurons in the *MrgprD*$^{-/-}$ group). These results imply that TRP-A1 is downstream of MrgprD in the same cell response.

MrgprD is functionally coupled to TRP-A1 in HEK293 cells

To verify the existence of functional coupling between MrgprD and TRP-A1, we chose the HEK293 cell line to coexpress MrgprD and TRP-A1 plasmids. The transfected cells ectopically expressed MrgprD and TRP-A1 proteins (**Fig. 6*B***). In the same experimental process as was described above, mustard oil and β-alanine were used to detect the coupling between TRP-A1 and MrgprD. As expected, β-alanine and mustard oil failed to trigger calcium influx in nontransfected HEK293 cells. However, β-alanine–induced calcium influx in HEK293 cells overexpressing both MrgprD, and TRP-A1 was greater than that in cells expressing MrgprD alone (Fig. 6*A*, *C*; 213 overexpressing both MrgprD and TRP-A1 cells and 208 expressing MrgprD alone were calculated). The amplitude of β-alanine–induced calcium influx in coexpressing MrgprD and TRP-A1 cells was consistently higher than that in cells expressing MrgprD alone (Fig. 6*D*). These data demonstrate that MrgprD is functionally coupled to TRP-A1.

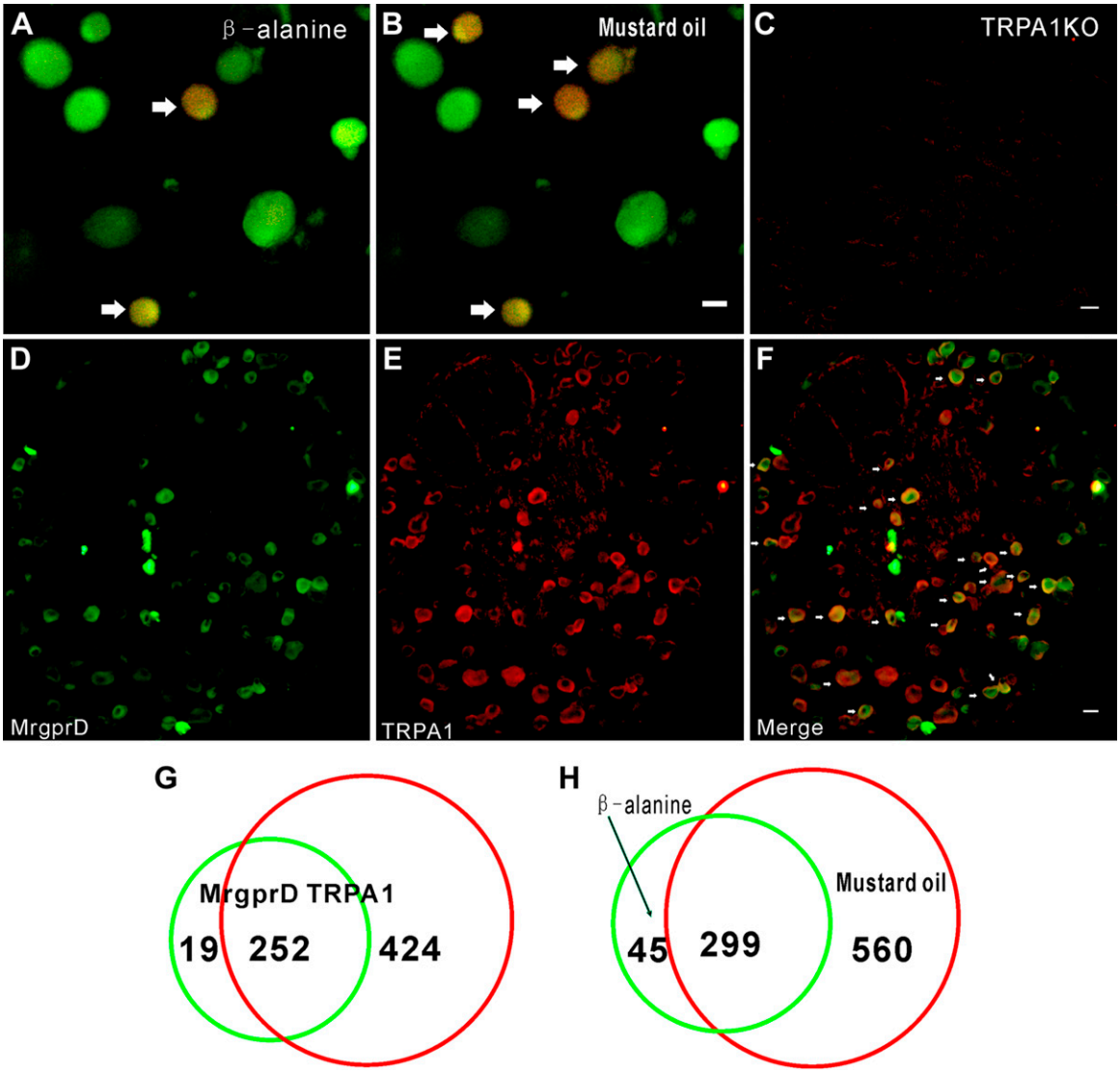

Figure 3. Most MrgprD$^+$ DRG neurons are TRP-A1$^+$. *A*, *B*) Representative images show DRG neurons responding to β-alanine (8 mM) and mustard oil (400 μM) in calcium imaging. Arrows: coresponsive cells. *C*) Immunostaining shows negative signal of TRP-A1 in DRG neurons from TRP-A1 KO mice. *D–F*) Immunofluorescence staining shows representative images of MrgprD$^+$ cells (*D*), TRP-A1$^+$ cells (*E*), and a merger of MrgprD$^+$ and TRP-A1$^+$ neurons (*F*). Arrows: double-labeled cells. *G*) Of 271 cells, 252 (92.9%) of MrgprD$^+$ cells were TRP-A1$^+$. *H*) Of 344 cells, 299 β-alanine (8 mM)–sensitive DRG neurons were coresponsive to mustard oil (400 μM). Scale bars, 20 μm.

MrgprD affects TRP-A1 function *via* the PKA pathway

As shown above, it has been found that MrgprD and TRP-A1 have some functional connections, but the signaling pathways between MrgprD and TRP-A1 remain elusive. To find out how MrgprD activation affects TRP-A1 function, we tested the effects of specific inhibitors to the PKA, PKC, and PLC pathway on the β-alanine–induced calcium influx. When DRG neurons were pretreated with H89 dihydrochloride (an inhibitor of PKA, 1 μM), β-alanine–induced calcium influx was significantly reduced. However, the inhibitors of PKC (chelerythrine chloride, 1 μM) and the inhibitors of PLC (U73122, 1 μM) did not exert significant effects on β-alanine-induced calcium influx (**Fig. 7*A–C***). Among all the investigated β-alanine–sensitive DRG neurons, H89 dihydrochloride inhibited 39.1 ± 6.3% of β-alanine–sensitive cells and showed a strong inhibitory effect (Fig. 7*E*; 2450 DRG neurons were counted, 367 cells responded to β-alanine, and 147 cells were inhibited), but only 8.4 ± 2.2 and 6.2 ± 6.4% of cells were suppressed to some extent by chelerythrine chloride and U73122 (Fig. 7*F*, *G*; of the 1057 DRG neurons counted, 162 cells responded to β-alanine in the chelerythrine chloride group, and of 993 DRG neurons analyzed, 147 cells responded to β-alanine in the U73122 group).

These observations indicate that the inhibition of PKA contributed greatly to the suppression of β-alanine–activated MrgprD signaling in DRG neurons. To confirm the role of the PKA pathway between the MrgprD and TRP-A1 channels, we repeated the above experiment in HEK293 cells; H89 dihydrochloride significantly inhibited β-alanine–induced calcium influx (Fig. 7*D*, *H*; 164 inhibited cells were counted, the fluorescence intensity of the second

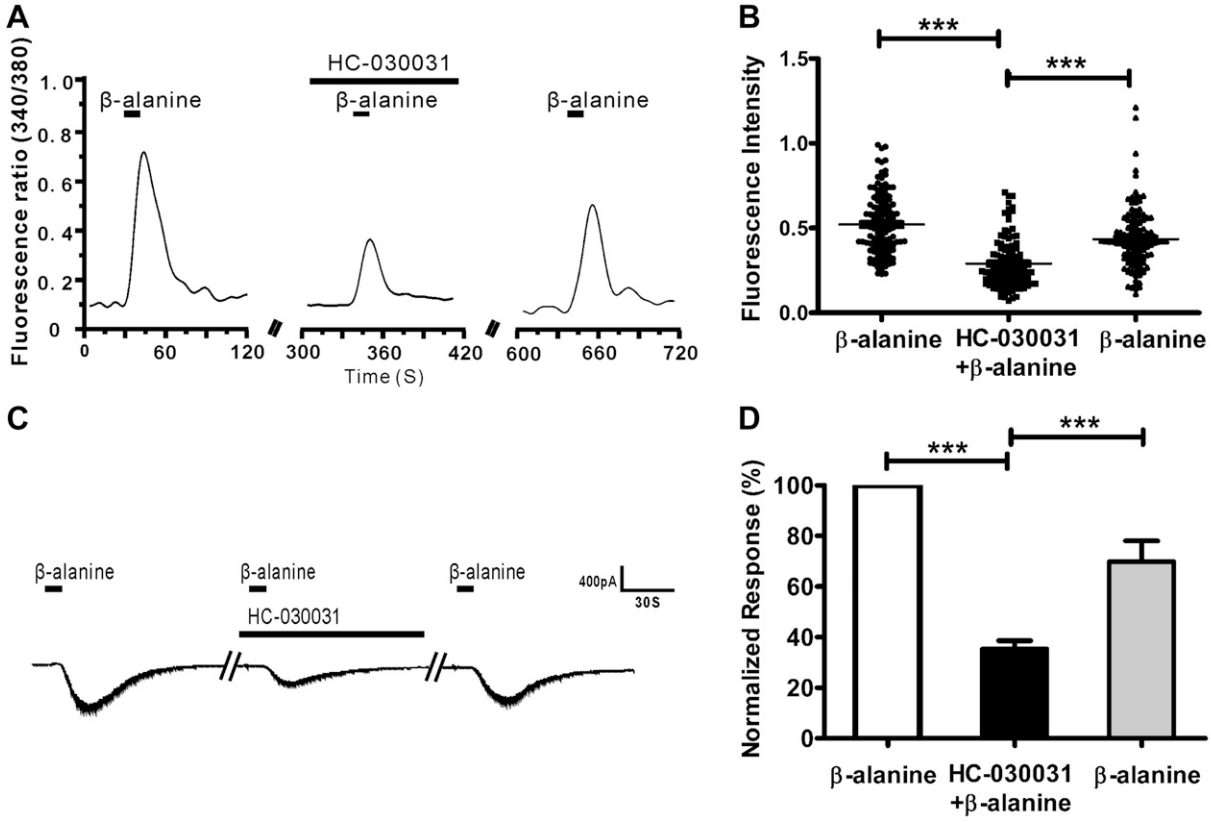

Figure 4. HC-030031 suppresses the β-alanine–induced response in DRG neurons. *A*) Representative traces show that β-alanine–induced calcium influx was reduced by pretreatment with HC-030031. *B*) The dot plots of the β-alanine–induced Ca^{2+} response indicate the inhibitory response of HC-030031 to β-alanine. *C*) Inward whole-cell currents induced by β-alanine (8 mM) in DRG neurons. HC-030031 suppressed the β-alanine–induced inward current. *D*) Nine neurons were recorded in each condition, and the inhibitory effect of HC-030031 on β-alanine–induced inward current was summarized in a histogram. ***$P <$ 0.001, by 1-way repeated-measures ANOVA.

application of β-alanine was lower than the third, and β-alanine induced calcium influx was significantly lower than that of the condition in the presence of H89 dihydrochloride. This indicated that β-alanine induced calcium influx was considered to be inhibited, indicating that PKA may be an important signaling pathway between MrgprD and the TRP-A1 channel.

The phosphorylation of TRP-A1 *via* the PKA pathway has been suggested to regulate its channel activity (26). Does the activation of MrgprD alter phosphorylation of TRP-A1? To be certain, a nanoimmunoassay was used to determine the phosphorylation status of TRP-A1. β-Alanine–induced activation of MrgprD led to the evident phosphorylation of TRP-A1 in DRG neurons, whereas the phosphorylation level of TRP-A1 was decreased by the pretreatment of H89 dihydrochloride (Fig. 7*I–L*), indicating MrgprD participated in TRP-A1 phosphorylation through activation of PKA.

β-Alanine induced more pain than itch in CCI models

Although β-alanine elicits itch-associated behavior through MrgprD (9, 11), MrgprD has been thought to be activated by nociceptive stimuli (27–29). Therefore, we sought to determine precisely the physiologic consequence of the β-alanine–activated MrgprD–TRP-A1 pathway in naive and CCI mice by testing the biting and licking behaviors in a lower hindlimb (calf) model to reflect itch and pain sensations, respectively (21–23, 30). We first detected the licking and biting behavior in WT mice by intraplantar injection of β-alanine (50 mM, 10 μl) and vehicle (saline, 10 μl). The number of licks and bites both increased compared with vehicle groups (Supplemental Fig. 3*A*, *B*; paired sample *t* tests, littermate control). The wiping and scratching behaviors were also examined by cheek injection of β-alanine (50 mM, 10 μl) and vehicle (saline, 10 μl). The number of both wiping bouts and scratching bouts differed from those in the vehicle groups (Supplemental Fig. 3*C*, *D*; paired sample *t* tests, littermate control). We found that, in comparison with WT mice, the levels of the intraplantar injection of β-alanine (50 mM, 10 μl) decreased both licking and biting in *MrgprD*$^{-/-}$ mice (**Fig. 8*A*, *B***). The results indicate that β-alanine induced pain and itch behaviors in non-CCI mice. Moreover, the β-alanine–induced licking and biting behaviors were tested in CCI models on d 7 and 14. In the WT mice, there were no significant differences in the biting behavior elicited by β-alanine between naive control and CCI mice (Fig. 8*C*). By contrast, the number of times licking on d 7 in the CCI group increased more

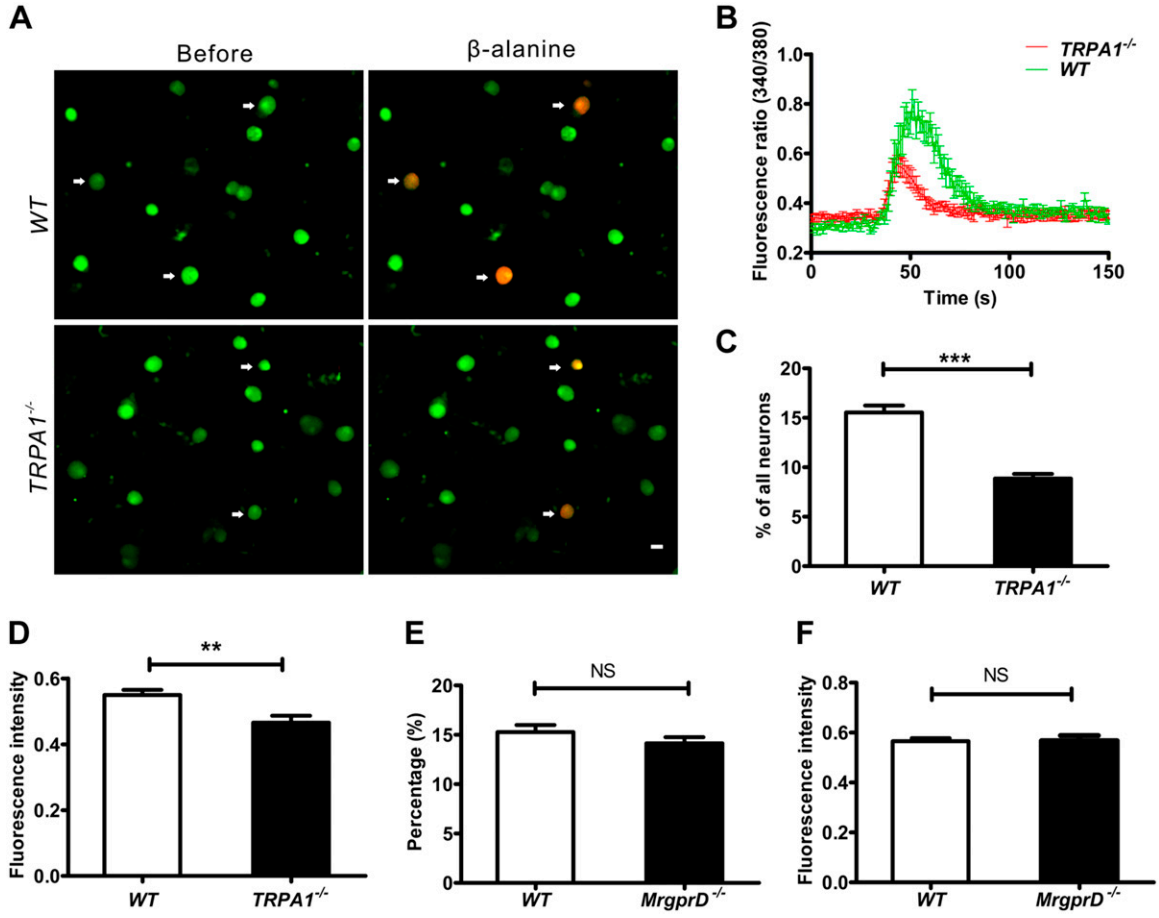

Figure 5. The β-alanine–induced response is decreased in TRP-A1-knockout mice. *A*) Fluorescent images of intracellular calcium flux induced by β-alanine. Arrows: neurons responsive to β-alanine in WT and *TRPA1*$^{-/-}$ DRGs. Scale bar, 20 μm. *B*) Representative fura-2 ratiometric responses in cultured DRG neurons. The curves show the responses of DRG neurons to β-alanine. *C*) The percentages of β-alanine–responsive neurons at the level of L4 DRGs from WT and *TRPA1*$^{-/-}$ mice (% of total neurons, $n = 3$ per group). *D*) The fluorescence intensities of β-alanine (8 mM)–induced calcium influx in DRG neurons of WT and *TRPA1*$^{-/-}$ mice ($n = 3$ per group). *E*) Percentages of mustard oil–responsive DRG neurons of WT and *MrgprD*$^{-/-}$ mice (% of total neurons, $n = 3$ per group). *F*) The fluorescence intensities of mustard oil–induced calcium influx in DRG neurons from WT and *MrgprD*$^{-/-}$ mice ($n = 3$ per group). ***$P < 0.001$, by independent samples *t* tests.

significantly than in naive mice (Fig. 8*D*). The ratio of licking behavior (the number of times biting compared to the sum of times licking and biting) was also significantly enhanced on d 7 and 14 after CCI (Fig. 8*E*). These observations indicate that β-alanine induced more pain than itch in the CCI model. Furthermore, the number of times biting and licking were compared in WT and *MrgprD*$^{-/-}$ mice after CCI. The times decreased in *MrgprD*$^{-/-}$ CCI mice, but the licking behavior changed much more than the biting behavior (Fig. 8*F*, *G*). Finally, *TRPA1*$^{-/-}$ mice were further used to confirm that TRP-A1 was involved in neuropathic pain with MrgprD. The licking behavior induced by β-alanine intraplantar injection was observed in *TRPA1*$^{-/-}$ mice before and after CCI. The number of times licking decreased slightly in *TRPA1*$^{-/-}$ mice compared with the WT mice without CCI (Fig. 8*H*); however, CCI led to more of a decrease in licking in *TRPA1*$^{-/-}$ mice than in WT mice (Fig. 8*I*). These results indicate that MrgprD is involved in both itching and pain. TRP-A1 facilitates the participation of MrgprD in neuropathic pain. In the CCI neuropathic pain model, β-alanine induced more pain than itching.

DISCUSSION

MrgprD was released for the first time as a member of the Mrgpr family in mice (6). Subsequently, a family of genes similar to the Mrgpr family was cloned in rats and humans, which was called MrgXs or sensory neuron-specific receptors (31, 32). Among the 4 subpopulations of the Mrgpr family, other subpopulations (MrgprA, -B, and -C) contain multiple members, except MrgprD (33). MrgprD has been identified as a subpopulation of nonpeptidergic nociceptive neurons. MrgprD fiber terminals have unique distribution characteristics, both at the periphery and the center (spinal cord). MrgprD^{+} fibers terminate in the stratum granulosum of the epidermis and are absent from specialized sensory structures. The central projections terminate in inner lamina II of the dorsal spinal cord (29). The specific pathway made up of MrgprD^{+} neurons may play an important role in some aspects of sensory information processing (10). A few years later, the results of an MrgprD functional study were also reported. Genetic ablation in adulthood of unmyelinated sensory neurons

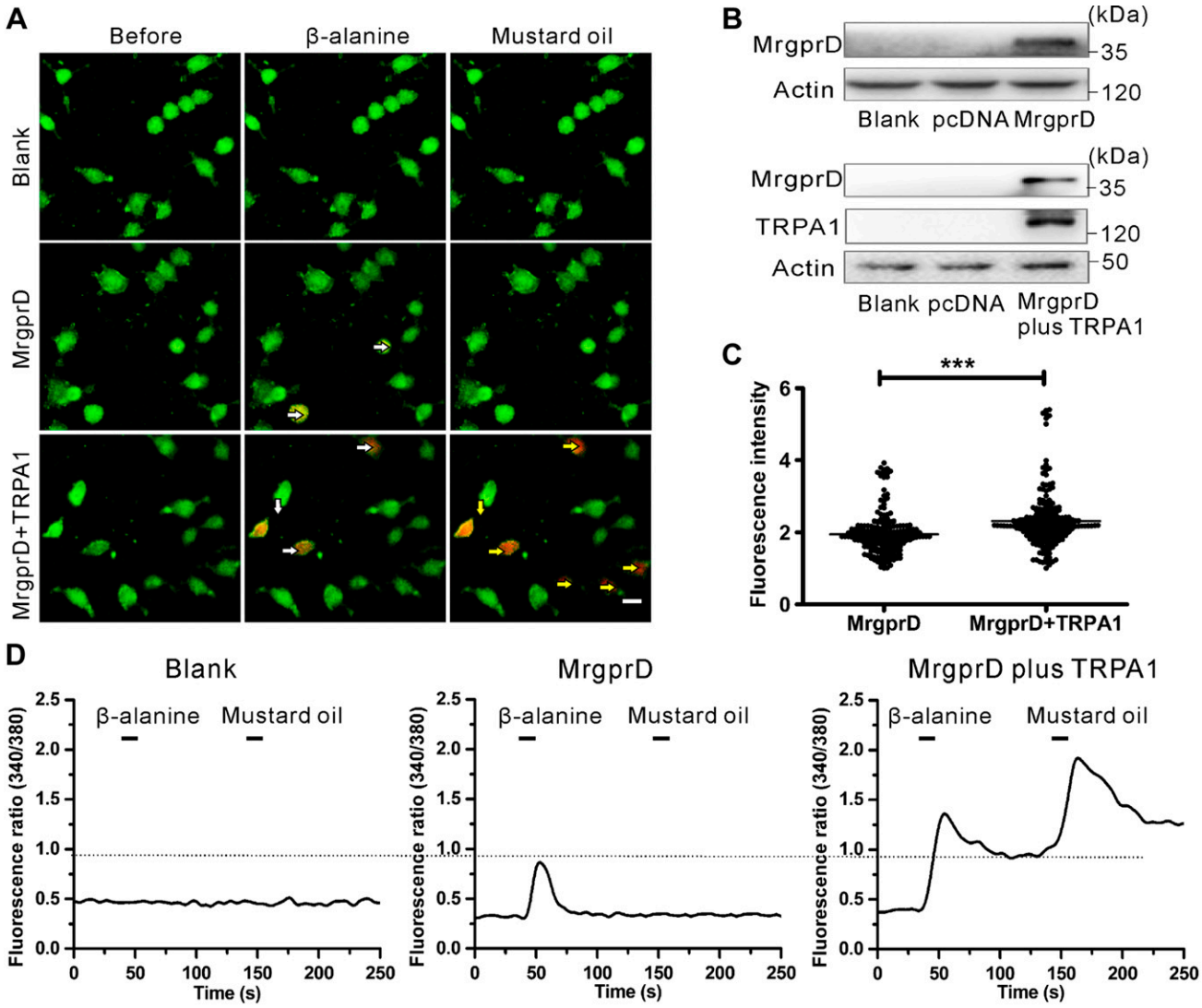

Figure 6. MrgprD is functionally associated with TRP-A1. *A*) Representative images of β-alanine–induced calcium responses. HEK293 cells were transfected with the expression plasmid of MrgprD (middle) or MrgprD combined with TRP-A1 (bottom). The cells were separately treated with β-alanine (8 mM) and mustard oil (400 μM). The nontransfected cells were used as the blank control. White arrows: β-alanine–responsive HEK293 cells overexpressing either MrgprD or MrgprD^{+} TRP-A1; yellow arrows: the mustard oil–responsive HEK293 cells with ectopic expression of MrgprD^{+} TRP-A1. Scale bar, 10 μm. *B*) Western blot analyses to verify the overexpression of MrgprD and TRP-A1 in transfected HEK293 cells. These cells were of the same transfected batch as was used for the images in *A*. *C*) The fluorescence intensities of β-alanine–induced calcium influx in MrgprD-expressing or MrgprD^{+} TRP-A- coexpressing cells (n = 3). ***$P < 0.001$, by independent samples t tests. *D*) Representative traces show β-alanine– and mustard oil–induced calcium responses in nontransfected (left), MrgprD-expressing (middle) and MrgprD^{+}TRP-A1–coexpressing (right) cells.

expressing the GPCR (MrgprD) reduces behavioral sensitivity to noxious mechanical stimuli but not to heat or cold stimuli (29). DRG neurons and fibers in mice lacking MrgprD exhibited decreased sensitivity to cold, heat, and mechanical stimuli, but *MrgprD*$^{-/-}$ mice did not exhibit any mechanical or thermal behavioral phenotype (28). In our experiments, *MrgprD*$^{-/-}$ and WT mice also did not show marked behavioral differences in response to mechanical, heat, and cold stimuli. However, in a neuropathic pain model (CCI), behavioral responses induced by mechanical stimulation between *MrgprD*$^{-/-}$ and WT mice differ considerably from those in nonpathologic conditions; in addition, significant behavioral differences were observed in cold but not heat stimulation between *MrgprD*$^{-/-}$ and WT mice. These results not only support the findings of other research groups, but further prove the important role of MrgprD in mechanical pain and cold pain in neuropathic conditions.

MrgprD has been thought to mediate noxious stimuli. In our study, the expression level of MrgprD increased in CCI mice, this result may be an important cause of the mechanical hyperalgesia and cold allodynia. The GPCR–TRP axis is an indispensable signaling pathway in sensing noxious, irritating, and inflammatory stimuli (5, 34). We found that the depletion of MrgprD significantly attenuated the CCI-induced cold allodynia. We therefore suppose that MrgprD could modulate a cold-sensing channel in DRG neurons. TRP

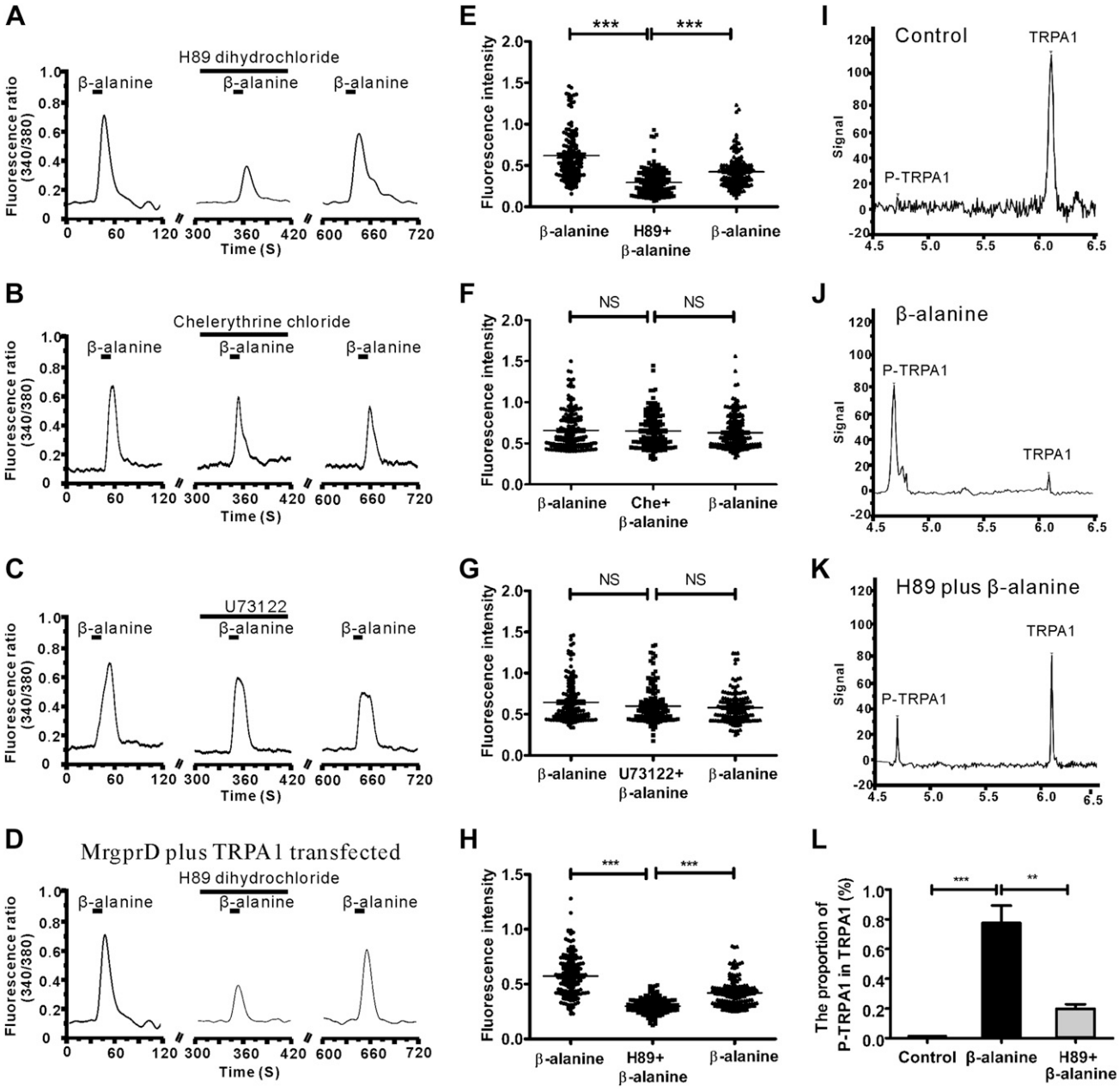

Figure 7. MrgprD signaling regulates TRP-A1 phosphorylation *via* PKA activation. *A–C*) Representative traces show that β-alanine (8 mM)–induced calcium influx in DRG neurons was reduced by pretreatment with H89 dihydrochloride (*A*), but was not substantially suppressed by pretreatment with chelerythrine chloride (*B*) or U73122 (*C*). *D*) Representative traces show β-alanine (8 mM)–induced calcium influx during the 3 consecutive treatments of β-alanine in MrgprD and TRP-A1 transfected HEK293 cells by the pretreatment with H89 dihydrochloride. *E*) The dot plots show that H89 dihydrochloride caused a substantial inhibition of the β-alanine–induced calcium signal. *F, G*) β-Alanine (8 mM)–induced calcium influx was not substantially suppressed by pretreatment with chelerythrine (*F*) chloride or U73122 (*G*). *H*) The dot plots show that H89 dihydrochloride caused a substantial inhibition of the β-alanine-induced calcium signal in MrgprD- and TRP-A1– transfected HEK293 cells. *I–K*) A nanoimmunoassay showed TRP-A1 phosphorylation in DRG neurons. Compared to the untreated control (*I*), treatment with β-alanine induced an increase in the phosphorylation of TRP-A1 in DRG neurons (*J*). By contrast, the β-alanine-induced phosphorylation of TRP-A1 was reduced with H89 pretreatment in DRG neurons (*K*). *L*) The phosphorylation levels of TRP-A1 in different conditions ($n = 3$ mice/group). $^{**}P < 0.01$; $^{***}P < 0.001$, by 1-way repeated-measures ANOVA.

channels are highly involved in the perception of neuropathic pain and in TRP-A1 mediation of neuropathic pain (35, 36). TRP-A1 contributes to cold, mechanical, and chemical nociception (mustard oil) (12, 34, 37). Therefore, we assumed that a cold-sensing TRP-A1 channel could be associated with MrgprD. Coexpression of MrgprD and TRP-A1 on DRG neurons provides the necessary conditions for a functional association between them.

β-Alanine was identified as the ligand of a GPCR named TGR7, which has been shown to be MrgprD (7, 11).

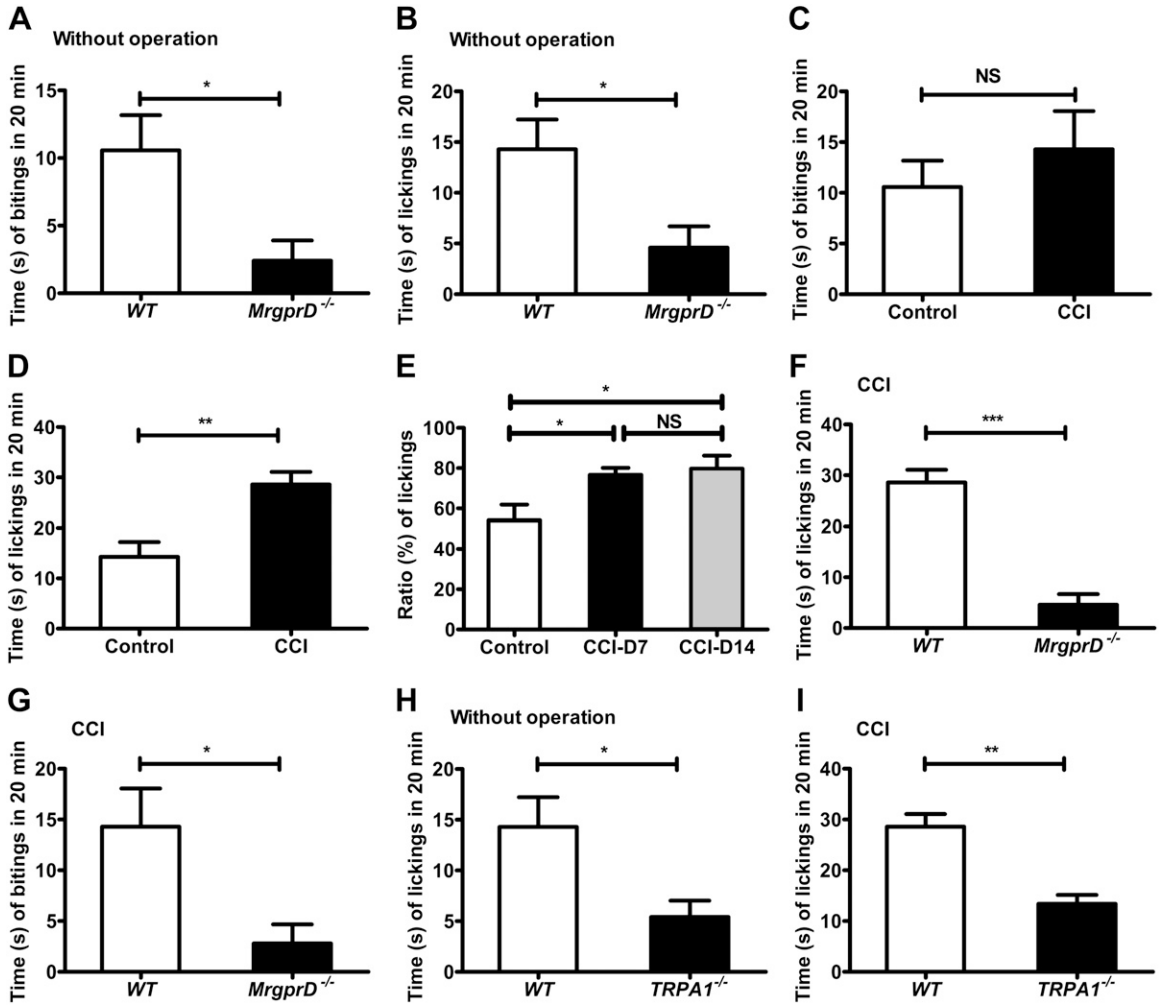

Figure 8. β-Alanine–induced more pain than itch in CCI models. *A*) The number of times biting in 20 min after injection of β-alanine (50 mM, 10 μl) in WT and *MrgprD*$^{-/-}$ mice without injury. *B*) The number of times licking in 20 min after injection of β-alanine (50 mM, 10 μl) in WT and *MrgprD*$^{-/-}$ mice without CCI. *C*) The biting behavior was unchanged between CCI models and controls after the injection of β-alanine (50 mM, 10 μl). *D*) The comparison of licking behavior after the injection of β-alanine (50 mM, 10 μl) between CCI models and controls. *E*) The mean ratio of licking behavior (the times biting compared to the sum of times licking and biting) in control mice after CCI for 7 d and in mice after CCI for 14 d. *F*) The times licking in 20 min after injection of β-alanine (50 mM, 10 μL) in WT and *MrgprD*$^{-/-}$ mice in CCI models. *G*) The times biting in 20 min after injection of β-alanine (50 mM, 10 μl) in WT and *MrgprD*$^{-/-}$ mice after CCI operation. *H*) The licking behavior after the injection of β-alanine (50 mM, 10 μl) in WT and *TRPA1*$^{-/-}$ mice without operation. *I*) Licking behavior after the injection of β-alanine (50 mM, 10 μl) in WT and *TRPA1*$^{-/-}$ mice after CCI ($n = 8$ for all experiments). $^{*}P < 0.05$, $^{**}P < 0.01$, $^{***}P < 0.001$, by (*A–D*, *F–I*) paired-sample Student's t-test, littermate control; (*E*) 1-way repeated-measures ANOVA.

β-Alanine specifically activates the MrgprD receptor, causing extracellular calcium influx and MrgprD^{+} neurons to become excited (38). β-Alanine induced calcium influx in DRG neurons after CCI was enhanced, suggesting that MrgprD activation is highly associated with calcium-mediated sensitization of DRG neurons. To demonstrate the functional relationship between MrgprD and TRP-A1, we used β-alanine to act on neurons in TRP-A1–knockout mice and found that β-alanine–induced calcium influx in TRP-A1–knockout DRG neurons was dramatically decreased, whereas there were no differences in mustard oil–induced calcium influx in MrgprD-knockout DRG neurons. In MrgprD and TRP-A1 transfected HEK293 cells, β-alanine–induced calcium influx in cells coexpressing MrgprD and TRP-A1 was higher than that in cells expressing MrgprD alone. Therefore, MrgprD and TRP-A1 have functional correlations, and this functional relationship becomes more pronounced in the CCI neuropathic model.

After stimulation, GPCRs activate the kinases in the downstream signaling pathway, such as cAMP-dependent PKA, PKC, or PLC, which leads to phosphorylation of TRP channels and increases the activity in response to endogenous agonists (5, 39). MrgprD interacts with its downstream mediators (Gαs/AC/cAMP), leading to an increase in the activity of PKA as its second messenger in primary aortic vascular smooth muscle cells (40). In our study, the antagonist of PKA (H89 dihydrochloride) obviously blocked most of the β-alanine–induced calcium signal in both DRG neurons and HEK293

cells transfected with MrgprD and TRP-A1, verifying that PKA is the main second-messenger kinase responsible for the transduction of MrgprD signaling. Moreover, we found that β-alanine–induced activation of MrgprD led to the enhanced phosphorylation levels of TRP-A1, which was suppressed by pretreatment with the antagonist of PKA. Therefore, we provide evidence that MrgprD activation induced by β-alanine regulates the TRP-A1 functions, at least in part, through PKA-mediated TRP-A1 phosphorylation.

In our previous work, β-alanine activated MrgprD and caused scratching behavior in cheek models (9, 11). In this study, β-alanine induced more pain than itch in CCI models, indicating that β-alanine–activated MrgprD signaling is involved in both the itching and pain sensations. MrgprD is more likely to participate in mechanical pain and cold allodynia in neuropathic pain. This study not only revealed the new function of MrgprD in pain, but also elucidated the new mechanism through the PKA signaling pathway. In this study, MrgprD is upstream of pain signaling; therefore, the inhibition of MrgprD is vital to attenuating neuropathic pain. Presently, researchers have not found the specific inhibitor of MrgprD. A metabolite that activates or inhibits MrgprD should improve the treatment of neuropathic pain. On the basis of these findings, MrgprD may be considered a new drug target for the treatment of neuropathic pain. FJ

ACKNOWLEDGMENTS

This work was supported by the National Science Foundation of China Grants 31471007 and 31771163 (to Z.T.) and 81600966 (to C.W.); the Natural Science Foundation of Jiangsu Province Grants 16KJB320005 (to C.W) and BK20151571 (to G.Y.); a Natural Science Fund Project of Colleges in Jiangsu Province Grant BK20161042 (to C.W.); and Jiangsu Keypoint Research and Invention Program Grant BE2017728 (to G.Y.). The project was funded by the Priority Academic Program Development of Jiangsu Higher Education Institutions (PAPD) and sponsored by a grant from the Qing Lan Project in Jiangsu Province (to Z.T.). This work was also supported by the Hunan Cooperative Innovation Center for Molecular Target New Drug Study, and Postdoctoral Science Foundation of China (M601863). C.W. and L.G. are co-senior authors. The authors declare no conflicts of interest.

AUTHOR CONTRIBUTIONS

C. Wang and L. Gu performed the experiments and statistical analyses; Y. Ruan, M. Xu, and N. Yang performed the behavior tests; X. Geng and L. Yu performed whole-cell recordings; Y. Jiang, C. Zhu, Y. Yang, X. Guan, and Y. Zhou helped breed the animals and participated in animal models and genotyping experiments; L. Lan performed the biochemistry experiment; W. Luo, Q. Liu, and X. Dong provided technical supports and *MrgprD*$^{-/-}$ mice; C. Wang, G. Yu, L. Lan, and Z. Tang conceived, designed, and planned the project; C. Wang and Z. Tang reviewed the statistical analyses and wrote the manuscript; C. Wang and L. Gu contributed equally to this work; and all authors read and approved the final manuscript.

REFERENCES

1. Haanpää, M., Attal, N., Backonja, M., Baron, R., Bennett, M., Bouhassira, D., Cruccu, G., Hansson, P., Haythornthwaite, J. A., Iannetti, G. D., Jensen, T. S., Kauppila, T., Nurmikko, T. J., Rice, A. S., Rowbotham, M., Serra, J., Sommer, C., Smith, B. H., and Treede, R. D. (2011) NeuPSIG guidelines on neuropathic pain assessment. *Pain* **152**, 14–27
2. Peng, J., Gu, N., Zhou, L., B Eyo, U., Murugan, M., Gan, W. B., and Wu, L. J. (2016) Microglia and monocytes synergistically promote the transition from acute to chronic pain after nerve injury. *Nat. Commun.* **7**, 12029
3. Nightingale, S. (2012) The neuropathic pain market. *Nat. Rev. Drug Discov.* **11**, 101–102
4. Van Hecke, O., Austin, S. K., Khan, R. A., Smith, B. H., and Torrance, N. (2014) Neuropathic pain in the general population: a systematic review of epidemiological studies. *Pain***155**, 654–662; correction: 1907
5. Veldhuis, N. A., Poole, D. P., Grace, M., McIntyre, P., and Bunnett, N. W. (2015) The G protein-coupled receptor-transient receptor potential channel axis: molecular insights for targeting disorders of sensation and inflammation. *Pharmacol. Rev.* **67**, 36–73
6. Dong, X., Han, S., Zylka, M. J., Simon, M. I., and Anderson, D. J. (2001) A diverse family of GPCRs expressed in specific subsets of nociceptive sensory neurons. *Cell* **106**, 619–632
7. Shinohara, T., Harada, M., Ogi, K., Maruyama, M., Fujii, R., Tanaka, H., Fukusumi, S., Komatsu, H., Hosoya, M., Noguchi, Y., Watanabe, T., Moriya, T., Itoh, Y., and Hinuma, S. (2004) Identification of a G protein-coupled receptor specifically responsive to beta-alanine. *J. Biol. Chem.* **279**, 23559–23564
8. Wooten, M., Weng, H. J., Hartke, T. V., Borzan, J., Klein, A. H., Turnquist, B., Dong, X., Meyer, R. A., and Ringkamp, M. (2014) Three functionally distinct classes of C-fibre nociceptors in primates. *Nat. Commun.* **5**, 4122
9. Liu, Q., and Dong, X. (2015) The role of the Mrgpr receptor family in itch. *Handb. Exp. Pharmacol.* **226**, 71–88
10. Zylka, M. J., Rice, F. L., and Anderson, D. J. (2005) Topographically distinct epidermal nociceptive circuits revealed by axonal tracers targeted to Mrgprd. *Neuron* **45**, 17–25
11. Liu, Q., Sikand, P., Ma, C., Tang, Z., Han, L., Li, Z., Sun, S., LaMotte, R. H., and Dong, X. (2012) Mechanisms of itch evoked by β-alanine. *J. Neurosci.* **32**, 14532–14537
12. Kwan, K. Y., Allchorne, A. J., Vollrath, M. A., Christensen, A. P., Zhang, D. S., Woolf, C. J., and Corey, D. P. (2006) TRPA1 contributes to cold, mechanical, and chemical nociception but is not essential for hair-cell transduction. *Neuron* **50**, 277–289
13. Bennett, G. J., and Xie, Y. K. (1988) A peripheral mononeuropathy in rat that produces disorders of pain sensation like those seen in man. *Pain* **33**, 87–107
14. Chaplan, S. R., Bach, F. W., Pogrel, J. W., Chung, J. M., and Yaksh, T. L. (1994) Quantitative assessment of tactile allodynia in the rat paw. *J. Neurosci. Methods* **53**, 55–63
15. Hargreaves, K., Dubner, R., Brown, F., Flores, C., and Joris, J. (1988) A new and sensitive method for measuring thermal nociception in cutaneous hyperalgesia. *Pain* **32**, 77–88
16. Farghaly, H. S., Mahmoud, A. M., and Abdel-Sater, K. A. (2016) Effect of dexmedetomidine and cold stress in a rat model of neuropathic pain: role of interleukin-6 and tumor necrosis factor-α. *Eur. J. Pharmacol.* **776**, 139–145
17. Wang, C., Wang, Z., Yang, Y., Zhu, C., Wu, G., Yu, G., Jian, T., Yang, N., Shi, H., Tang, M., He, Q., Lan, L., Liu, Q., Guan, Y., Dong, X., Duan, J., and Tang, Z. (2015) Pirt contributes to uterine contraction-induced pain in mice. *Mol. Pain* **11**, 57
18. Kim, A. Y., Tang, Z., Liu, Q., Patel, K. N., Maag, D., Geng, Y., and Dong, X. (2008) Pirt, a phosphoinositide-binding protein, functions as a regulatory subunit of TRPV1. *Cell* **133**, 475–485
19. Liu, Q., Tang, Z., Surdenikova, L., Kim, S., Patel, K. N., Kim, A., Ru, F., Guan, Y., Weng, H. J., Geng, Y., Undem, B. J., Kollarik, M., Chen, Z. F., Anderson, D. J., and Dong, X. (2009) Sensory neuron-specific GPCR Mrgprs are itch receptors mediating chloroquine-induced pruritus. *Cell* **139**, 1353–1365
20. Ma, W., Zhang, Y., Bantel, C., and Eisenach, J. C. (2005) Medium and large injured dorsal root ganglion cells increase TRPV-1, accompanied by increased α2C-adrenoceptor co-expression and functional inhibition by clonidine. *Pain* **113**, 386–394

21. Akiyama, T., Nagamine, M., Carstens, M. I., and Carstens, E. (2014) Behavioral model of itch, alloknesis, pain and allodynia in the lower hindlimb and correlative responses of lumbar dorsal horn neurons in the mouse. *Neuroscience* **266**, 38–46
22. Qu, L., Fan, N., Ma, C., Wang, T., Han, L., Fu, K., Wang, Y., Shimada, S. G., Dong, X., and LaMotte, R. H. (2014) Enhanced excitability of MRGPRA3- and MRGPRD-positive nociceptors in a model of inflammatory itch and pain. *Brain* **137**, 1039–1050
23. Foster, E., Wildner, H., Tudeau, L., Haueter, S., Ralvenius, W. T., Jegen, M., Johannssen, H., Hösli, L., Haenraets, K., Ghanem, A., Conzelmann, K. K., Bösl, M., and Zeilhofer, H. U. (2015) Targeted ablation, silencing, and activation establish glycinergic dorsal horn neurons as key components of a spinal gate for pain and itch. *Neuron* **85**, 1289–1304
24. Shimada, S. G., and LaMotte, R. H. (2008) Behavioral differentiation between itch and pain in mouse. *Pain* **139**, 681–687
25. Ajit, S. K., Pausch, M. H., Kennedy, J. D., and Kaftan, E. J. (2010) Development of a FLIPR assay for the simultaneous identification of MrgD agonists and antagonists from a single screen. *J. Biomed. Biotechnol.* **2010**, 326020
26. Meents, J. E., Fischer, M. J., and McNaughton, P. A. (2017) Sensitization of TRPA1 by protein kinase A. *PLoS One* **12**, e0170097
27. Vrontou, S., Wong, A. M., Rau, K. K., Koerber, H. R., and Anderson, D. J. (2013) Genetic identification of C fibres that detect massage-like stroking of hairy skin in vivo. *Nature* **493**, 669–673
28. Rau, K. K., McIlwrath, S. L., Wang, H., Lawson, J. J., Jankowski, M. P., Zylka, M. J., Anderson, D. J., and Koerber, H. R. (2009) Mrgprd enhances excitability in specific populations of cutaneous murine polymodal nociceptors. *J. Neurosci.* **29**, 8612–8619
29. Cavanaugh, D. J., Lee, H., Lo, L., Shields, S. D., Zylka, M. J., Basbaum, A. I., and Anderson, D. J. (2009) Distinct subsets of unmyelinated primary sensory fibers mediate behavioral responses to noxious thermal and mechanical stimuli [published correction appears in *Proc. Natl. Acad. Sci. USA* 106, 11424]. *Proc. Natl. Acad. Sci. USA* **106**, 9075–9080
30. LaMotte, R. H., Shimada, S. G., and Sikand, P. (2011) Mouse models of acute, chemical itch and pain in humans. *Exp. Dermatol.* **20**, 778–782
31. Bender, E., Buist, A., Jurzak, M., Langlois, X., Baggerman, G., Verhasselt, P., Ercken, M., Guo, H. Q., Wintmolders, C., Van den Wyngaert, I., Van Oers, I., Schoofs, L., and Luyten, W. (2002) Characterization of an orphan G protein-coupled receptor localized in the dorsal root ganglia reveals adenine as a signaling molecule. *Proc. Natl. Acad. Sci. USA* **99**, 8573–8578
32. Lembo, P. M., Grazzini, E., Groblewski, T., O'Donnell, D., Roy, M. O., Zhang, J., Hoffert, C., Cao, J., Schmidt, R., Pelletier, M., Labarre, M., Gosselin, M., Fortin, Y., Banville, D., Shen, S. H., Ström, P., Payza, K., Dray, A., Walker, P., and Ahmad, S. (2002) Proenkephalin A gene products activate a new family of sensory neuron–specific GPCRs. *Nat. Neurosci.* **5**, 201–209
33. Zylka, M. J., Dong, X., Southwell, A. L., and Anderson, D. J. (2003) Atypical expansion in mice of the sensory neuron-specific Mrg G protein-coupled receptor family. *Proc. Natl. Acad. Sci. USA* **100**, 10043–10048
34. Wilson, S. R., Gerhold, K. A., Bifolck-Fisher, A., Liu, Q., Patel, K. N., Dong, X., and Bautista, D. M. (2011) TRPA1 is required for histamine-independent, Mas-related G protein-coupled receptor-mediated itch. *Nat. Neurosci.* **14**, 595–602
35. Trevisan, G., Benemei, S., Materazzi, S., De Logu, F., De Siena, G., Fusi, C., Fortes Rossato, M., Coppi, E., Marone, I. M., Ferreira, J., Geppetti, P., and Nassini, R. (2016) TRPA1 mediates trigeminal neuropathic pain in mice downstream of monocytes/macrophages and oxidative stress. *Brain* **139**, 1361–1377
36. Basso, L., and Altier, C. (2017) Transient receptor potential channels in neuropathic pain. *Curr. Opin. Pharmacol.* **32**, 9–15
37. Karashima, Y., Talavera, K., Everaerts, W., Janssens, A., Kwan, K. Y., Vennekens, R., Nilius, B., and Voets, T. (2009) TRPA1 acts as a cold sensor in vitro and in vivo. *Proc. Natl. Acad. Sci. USA* **106**, 1273–1278
38. Zhuo, R. G., Ma, X. Y., Zhou, P. L., Liu, X. Y., Zhang, K., Wei, X. L., Yan, H. T., Xu, J. P., and Zheng, J. Q. (2014) Mas-related G protein-coupled receptor D is coupled to endogenous calcium-activated chloride channel in Xenopus oocytes. *J. Physiol. Biochem.* **70**, 185–191
39. Petho, G., and Reeh, P. W. (2012) Sensory and signaling mechanisms of bradykinin, eicosanoids, platelet-activating factor, and nitric oxide in peripheral nociceptors. *Physiol. Rev.* **92**, 1699–1775
40. Tetzner, A., Gebolys, K., Meinert, C., Klein, S., Uhlich, A., Trebicka, J., Villacañas, Ó., and Walther, T. (2016) G-protein-coupled receptor MrgD is a receptor for angiotensin-(1-7) involving adenylyl cyclase, cAMP, and phosphokinase A. *Hypertension* **68**, 185–194

Received for publication April 1, 2018.
Accepted for publication July 30, 2018.